

PAPER • OPEN ACCESS

Blue luminescence of indium-doped ZnO thin films prepared by DC magnetron sputtering

To cite this article: S Sugianto *et al* 2021 *J. Phys.: Conf. Ser.* **1968** 012045

View the [article online](#) for updates and enhancements.

You may also like

- [Solution-processed undoped and Indium doped ZnO thin film transistors: role of Ag nanowires into InZnO channel layer](#)
Manoj Kumar, Hakyung Jeong and Dongjin Lee
- [Physical properties of indium zinc oxide and aluminium zinc oxide thin films deposited by radio-frequency magnetron sputtering](#)
Nicoleta Vasile, Sorina Iftimie, Tomy Acscnte *et al.*
- [Boosting highly transparent and conducting indium zinc oxide thin films through solution combustion synthesis: influence of rapid thermal annealing](#)
Sana Ullah, Rita Branquinho, Ana Santa *et al.*



244th Electrochemical Society Meeting

October 8 – 12, 2023 • Gothenburg, Sweden

50 symposia in electrochemistry & solid state science

▶ **Deadline Extended!**
Last chance to submit!

New deadline:
April 21
submit your abstract!

Blue luminescence of indium-doped ZnO thin films prepared by DC magnetron sputtering

S Sugianto^{1,*}, N Nurilhilmah¹, T Darsono¹, S Sugiyanto¹, D Aryanto² and I Isnaeni²

¹ Department of Physics, Faculty of Mathematics and Natural Sciences, Universitas Negeri Semarang, Jl. Raya Sekaran Gunungpati 50299, Indonesia

² Research Center for Physics, Indonesian Institute of Sciences, Puspitek Serpong Gd 440-442 Tangerang Selatan, Indonesia

*sugianto@mail.unnes.ac.id

Abstract. ZnO is an intrinsic semiconductor suitable for many optical applications. In this current study homemade DC magnetron sputtering was used to grow undoped ZnO and indium-doped ZnO (or IZO) thin films. The indium content was varied from a mole fraction ratio of In₂O₃ were 0 at% to 6 at%. The structure of IZO films analyzed by X-ray diffraction (XRD), and the optical properties were carried out using UV-visible and photoluminescence (PL) spectroscopies. The XRD results demonstrated that IZO maintained a hexagonal wurtzite structure with a (002) preferential orientation. The optical band gap increased with an increase in indium doped concentration. The PL spectrum exhibits a broadband blue emission from IZO films centered at 440 nm (2.82 eV), originating from the radiative recombination at the defect level. Interestingly, the intensity of blue emission increased with an increase in indium-doped concentration.

1. Introduction

ZnO is one of the II-VI semiconductor materials with hexagonal close packing and has a wurtzite structure with P6₃mc symmetry. The lattice constants of ZnO are $a = 3.2539 \text{ \AA}$ and $c = 5.2098 \text{ \AA}$. ZnO is an *n*-type semiconductor material with a direct wide band gap of 3.37 eV and a high excitation binding of the energy of 60 meV, which can provide efficient excitonic emission at room temperature. Therefore, ZnO is considered one of the promising semiconducting materials for a wide range of application in the blue and UV optoelectronics devices such as blue/UV light-emitting diodes (LEDs) [1], lasers diodes (LDs) [2] and photodetectors [3]. ZnO films with high intensity photoemission have been extensively deposited by several growth techniques, such as pulse laser deposition (PLD) [4], metal-organic chemical vapor deposition (MOCVD) [5], pyrolysis [6], sol-gel spin coating [7], and rf sputtering [8].

Doping of ZnO with suitable dopant was well-known method for achieving the desired material properties. In general, doping in wide band gap semiconductors often caused changes in the optical and electric properties. For this purpose, it can be improved by a selective doping substituting Zn with higher valence element such as aluminum, gallium, and indium [9-12]. Studies on the photoluminescence of undoped ZnO films have been carried out by researchers [13-15], and they report that the ZnO has two emission bands, namely an ultraviolet band (360-390 nm) related to exciton and a visible band (405-700 nm) related to structural defect. Han et al [16] reported that the characteristic of defect on ZnO could



determine the light emitted color. Oxygen vacancies were major defect in the hexagonal cones, producing green emission (~ 500 nm). This paper reports the blue emission of indium-doped ZnO (or IZO) films grown using homemade DC magnetron sputtering. The impact of indium-doping concentration on structural and optical properties was considered.

2. Experimental methods

Homemade DC magnetron sputtering was used to grow undoped ZnO and IZO thin films. The stages of thin film growth begin with the makes of IZO targets, substrate preparation, and the growth of IZO thin films. IZO sputtering target of 2 inches in diameter was prepared using raw materials ZnO (99.99%) and In_2O_3 (99.99%), the total mass of the IZO target of 10 gr with a mole fraction ratio of In_2O_3 were 0%, 2%, 4% and 6%, respectively. The mixture of ZnO and In_2O_3 was synthesized using a solid-state reaction, calcined at 500 °C for 4 hours, and sintered at 750 °C for 5 hours. IZO thin films were grown on a corning glass substrate. Substrate preparation as described in previous studies [17]. Before the IZO film's growth, the sputtering reactor was vacuumed to a pressure of 1 mTorr, and then argon gas flowed up to pressure deposition of about 500 mTorr. IZO films were grown at a temperature of 400 °C with 30 W plasma power for 120 min. The X-ray powder diffraction (XRD) analysis was carried out to investigate the crystal structure of undoped ZnO and IZO films. UV-vis spectrophotometer and photoluminescence (PL) at room temperature were used to analyze the optical properties of undoped ZnO and IZO films.

3. Results and discussion

The structural analysis of IZO films were carried out using XRD with a $\text{CuK}\alpha$ ($\lambda = 1.5406 \text{ \AA}$) as an X-ray source. Figure 1 illustrates the XRD pattern of undoped and In-doped ZnO films. The sharp diffraction peaks manifest that ZnO have high crystallinity. All the XRD peaks are well-matched with ZnO's standard hexagonal wurtzite structure (JCPDS, No. ICDD-00-005-0664), and no characteristic peak of other impurities were observed. The undoped ZnO film has 5 main diffraction peaks at $2\theta = 34,36^\circ$; $36,24^\circ$; $47,44^\circ$; $62,64^\circ$; and $67,96^\circ$ corresponding to the crystal of (002), (101), (102), (103), dan (112) plane, respectively. The ZnO film grows to form polycrystalline structure with a dominant peak at the (002) plane. After doped with indium, IZO films with a concentration of indium 2 at% and 4 at% tended to grow in the direction of (002) plane. The full-width at half-maximum (FWHM) of the (002) diffraction peak gets wider when the indium concentration increases of 4%. The peak of (002) plane disappeared when the indium increases by 6 at% and this film appeared amorphous. All above indicate that the ZnO crystal's growth orientation is obviously influenced by the incorporation of indium, there are the indium atoms substitute Zn atoms in hexagonal and In^{3+} lattices can be interstitial sites ZnO.

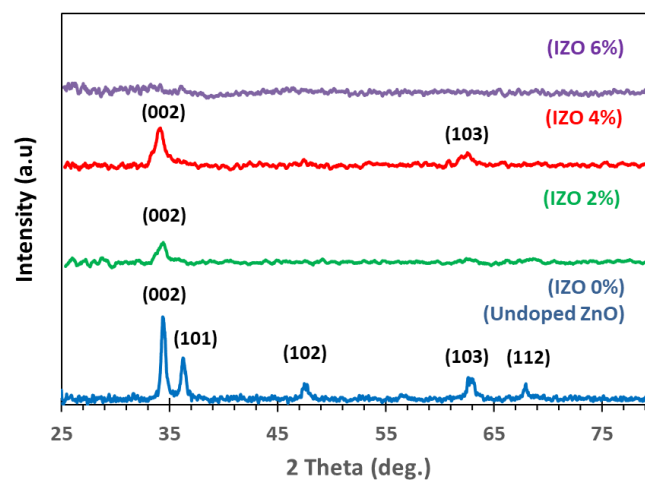


Figure 1: X-ray diffraction patterns of undoped ZnO and indium-doped ZnO films.

The lattice parameters, d -spacing, and crystalline size (D) are calculated from the XRD data shown in Table 1. A small shift in the position of the main peak (002) to the lower side of 2θ value and broadening of (002) peak were observed in the indium-doped ZnO samples (IZO 2 at% and 4 at%), due to larger ionic radius of In^{3+} (80 pm) than that of Zn^{2+} (74 pm), so that the lattice expands and the lattice parameters increases when indium ionic replace Zn ionic in the ZnO lattice. We have carried out the particle's average crystallite size (D) for each reflection by Scherrer's formula [18]. The average crystallite of IZO samples (In 2 at% of 9.45 nm and in 4 at% of 8.94 nm) are found to be smaller when compared to the undoped ZnO film (19.35 nm). A broadening of wurtzite ZnO peaks supports the decrease of crystallite sizes by increasing indium content and incorporating indium into the lattice. The smallest crystal size is obtained for the IZO 4 at% film (8.94 nm).

Table 1: The parameter of crystal structure for IZO films: 0 at%, 2 at%, 4 at%, and 6at%.

Indium Conc. (%)	hkl	2θ ($^\circ$)	FWHM ($^\circ$)	c (\AA)	d -spacing (\AA)	D (nm)
0	002	34.36	0.43	5.212	2.606	19.35
2	002	34.32	0.88	5.218	2.609	9.45
4	002	34.14	0.93	5.246	2.623	8.94
6	-	-	-	-	-	-

UV-vis spectrophotometer analysis has been carried out to investigate the optical properties of the IZO films, that are the transmittance and band gap energy. Figure 2 shows the UV-vis spectra of the IZO films 0 at%, 2 at%, 4 at%, and 6 at%. It indicates that IZO film's transmittance is related to the crystalline quality and crystalline size of each film based on UV-vis spectrophotometer data. The average transmittance of IZO films in the visible wavelength range can be seen in Table 1. Undoped ZnO film has good transparency in the visible range of about 87.2%, while the transmittance of IZO films is highly dependent on the concentration of indium doping and film crystallinity. When the indium's doping concentration is 4 at%, the transmittance is 88.5% better than undoped ZnO. The increase of transmittance may due to the decrease of optical scattering caused by the densification of grains and reduction of grain size as shown in Table 1. However, the transmittance decreased to 78.5% when the doping concentration is increased to 6 at%. Hafdallah et al [19] also reported a deterioration of transparency with increasing indium concentration.

Additionally, the IZO films exhibited a high absorption in the ultraviolet range from the recorded transmission spectra. The high absorption in the ultraviolet range is related to the fundamental absorption, which can be used to determine the optical band gap (E_g) of the semiconductor. The optical bandgap of the IZO films can be determined by the Touc Plot [20] method, namely by linearly extrapolating the graph of the absorption coefficient $(\alpha h\nu)^2$ and $h\nu$ (eV) as shown in Figure 3. The relationship between the absorption coefficient and band gap energy shown by the following equation:

$$\alpha h\nu = A (h\nu - E_g)^{(1/2)} \quad (1)$$

The optical band gap of IZO films with various doping concentrations of indium can be seen in Table 2. The optical band gap of IZO films is very dependent on the doping concentration of indium in ZnO film. IZO films with the doping concentrations of indium are 0 at%, 2 at%, and 4 at% have an increasing optical band gap are 3.19 eV, 3, 21 eV, and 3.80 eV, respectively. The increasing of the optical band gap with the doping impurities is mainly due to distortions in the crystal structure by the incorporation of doping impurities. This result is in agreement with the changes observed in the XRD pattern. The increase in the optical band gap value could also be due to an increase in carrier concentration or crystal defects associated with the Burstein-Moss effect. These results are consistent with previous studies [21, 22]. Meanwhile, there is a decrease in the band gap in the IZO 6 at% to 3.16 eV, may be related to its amorphous crystal quality.

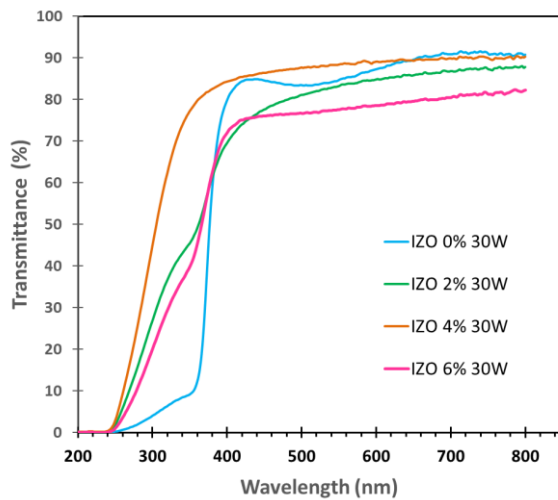


Figure 2. Transmission spectra of undoped ZnO and indium-doped ZnO films.

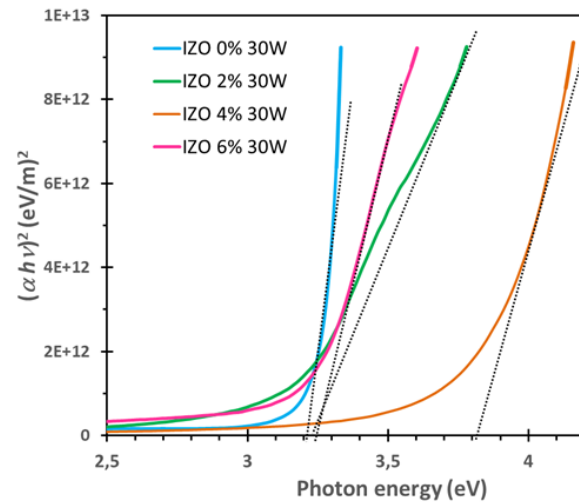


Figure 3. Tauc's plot of undoped ZnO and indium-doped ZnO films.

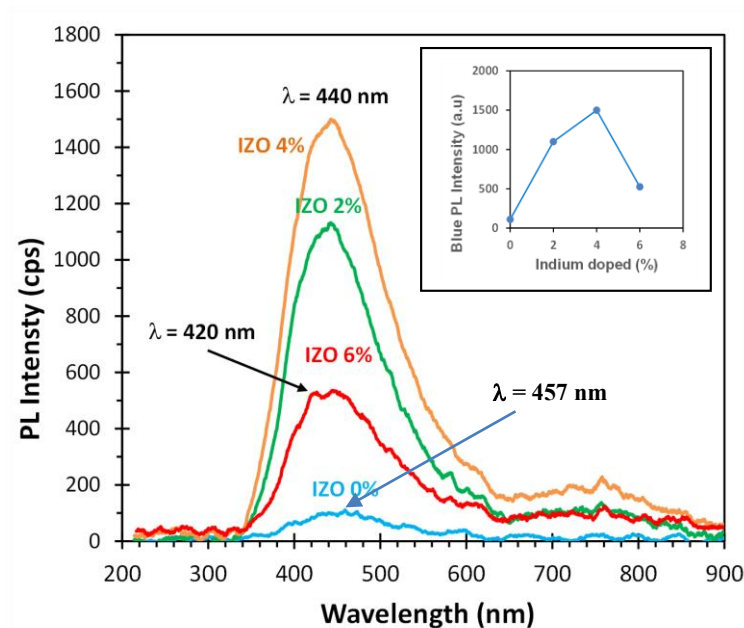


Figure 4. Photoluminescence spectra of undoped ZnO and indium-doped ZnO thin films at room temperature.

Figure 4 shows the photoluminescence (PL) spectra of undoped ZnO and indium-doped ZnO thin films by a 325 nm excitation at room temperature. PL spectra of the undoped ZnO film showed a weak and broad band PL peak extending from the UV to the visible region (340 nm to 600 nm). The characteristics of PL undoped ZnO film are similar to those studied by Thapa et al. [23]. It can be explained that the broad band PL shows the occurrence of UV emission and visible light emission from ZnO film. According to the band-edge emission in ZnO, the UV PL is attributed to the band gap of the ZnO film (~ 3.19 eV) in this study. As can be seen in Figure 4, the PL peak of this undoped ZnO film centered at a wavelength of ~ 457 nm will be referred to as the blue emission. This blue emission PL presumably

originates from electron-hole recombination mediated by defect levels such as zinc interstitials (Zn_i) present in ZnO. The presence of this defect in the ZnO film is related to the sputtering method which tends to produce ZnO thin films under Zn-rich conditions [23]. When ZnO was doped with indium, the intensity of the PL peak of IZO films increased compared to the undoped ZnO and the PL peak shifted towards the UV region at a shorter wavelength of 440 nm, which may be ascribed to the incorporation of indium. Blue emission band (440 nm or 2.82 eV) is generated by the electron transition from shallow donor (indium) level formed by interstitial Zn atoms to the top of the valence band. PL peaks of IZO film at a wavelength of 420 nm appear when the doping concentration of indium is increased to 6 at%, but the peak intensity is lower due to poor crystal quality.

4. Conclusion

Undoped ZnO and indium-doped ZnO (IZO) films were prepared by DC magnetron sputtering. The structural and optical properties of IZO films depend on the indium dopant content. IZO films with indium of 2 at% and 4 at% have a hexagonal wurtzite crystal structure, whereas IZO film with 6 % has an amorphous structure. IZO films with a concentration of indium 2 at% and 4 at% tended to grow in the direction of (002) plane. IZO films have higher transmittance than ZnO, which is around 87.5%. The optical band gap of IZO film also increased with an increase in indium doped concentration. The PL spectra exhibits a broad blue emission from IZO films centered at 440 nm (2,82 eV) generated by the electron transition from shallow donor level formed by interstitial Zn atoms to the top valence band). The intensity of blue emission increased with an increase in indium-doped concentration. This IZO films prepared by DC magnetron sputtering may promise for application to the blue light-emitting device.

Acknowledgement

The paper is supported by DIPA UNNES Fundamental Research programmer under grant agreement number: 68.31.5/UN37/PPK.4.4/2019.

References

- [1] Rahman F 2019 *Optical Engineering* **58** 010901
- [2] Liu C Y, Xu H Y, Sun Y, Ma J G, and Liu Y C 2014 *Optics Express* **22** 16731
- [3] Khokhra R, Bharti B, Lee H N, and Kumar R 2017 *Scientific Reports* **7** 15032
- [4] Tian K, Tudu B, and Tiwari A 2017 *Vacuum* **146** 483
- [5] Wu B, Zhuang S W, Chi C, Shi Z F, Jiang J Y, Dong X, Li W C, Zhang Y T, Zhang B L, and Duab G T 2016 *Phys. Chem. Chem. Phys.* **18** 5614
- [6] Mansour S, Farha A, and Kotkata M 2017 *Int J Appl Ceram Technol.* **14** 1213
- [7] Chebil W, Boukadhaha M A, and Fouzri A 2016 *Superlattices and Microstructures* **95** 48
- [8] Jazmatia A K, Abdallaha B 2018 *Materials Research* **21** 20170821
- [9] Tarwal N L, Rajgure A V, Inamdar A I, Devane R S, Kim I Y, Suryavanshi S, Ma Y R, Kim J H, and Patil P S 2013 *Sensors and Actuators A* **199** 67
- [10] Marinova G, Lovchinova K, Madjarova V, Strijkova V, Vasileva M, Malinowski N, and Babeva T 2019 *Optical Materials* **89** 390
- [11] Muchuweni E, Sathiaraj T S, and Nyakoty H 2016 *Ceramics International* **42** 10066
- [12] Farid S, Mukherjee S, Sarkar K, Stroschio M A, and Dutta M 2019 *J. Phys. Chem. A* **123** 8690
- [13] Janotti A, and Walle V D 2007 *Phys.Rev. B: Condens. Matter. Phys.* **76** 165202
- [14] Damberga D, Viter R, Fedoremco V, Iatsunskyi I, Coy E, Graniel O, Balme S, Miele P, and Bechelany M 2020 *Phys. Chem. C* **124** 9434
- [15] Jangir K J, Kumari Y, Kumar A, Kumar M, and Awasthi K 2017 *Mater. Chem. Front.* **1** 1413
- [16] Han N S, Shim H S, Seo J H, Kim S Y, Park S M, and Song J K 2010 *J. of Appl. Phys.* **107** 084306
- [17] Sugianto S, Astuti B, Marwoto P, Firmahaya N A, Aryanto D, and Isnaeni 2020 *Journal of Physics: Conference Series* **1567** 022003
- [18] Cullity B D, and Stock S R 2001 *Elements of X-ray Diffractions vol.3* (Prentice Hall, Engle-wood Cliffs)

- [19] Hafdallah A, Yanineb F, Aida M S, and Attaf N 2011 *J. of Alloys and Compounds* **509** 7267
- [20] Fu C F, Han L F, and Liu C 2015 *J. Mater. Sci: Mater Electron* **26** 493
- [21] Xie G C, Fang L, Peng L P, Liu G B, Ruan H B, Wu F, Kong C Y 2012 *Physics Procedia* **32** 651
- [22] Sugumaran S, Bellan C S, and Bheeman D 2017 *Optical Materials* **72** 618e625
- [23] Thapa D, Huso J, Morrison J L, Corolewski C D, McClusky M D, and Bergman L 2016 *Optical Materials* **58** 382